A Key to Improved Ion Core Confinement in the JET Tokamak: Ion Stiffness Mitigation due to Combined Plasma Rotation and Low Magnetic Shear

P.Mantica 1), C.Angioni 2), B.Baiocchi 1),3), C.Challis 4), J.Citrin 5), G.Colyer 4), A.C.A.Figueiredo 6), L.Frassinetti 7), E.Joffrin 8),9), T.Johnson 7), E.Lerche 10), A.G.Peeters 11), A.Salmi 12), D.Strintzi 13), T.Tala 14), M.Tsalas 13),9), D.Van Eester 10), P.C.deVries 5), J.Weiland 15), M.Baruzzo 16), M.N.A.Beurskens 4), J.P.S.Bizarro 6), P.Buratti 17), F.Crisanti 17), X.Garbet 8), C.Giroud 4), N.Hawkes 4), J. Hobirk 2), F.Imbeaux 8), J.Mailloux 4), V.Naulin 1), C.Sozzi 1), G.Staebler 19), T.W.Versloot 5), and JET EFDA contributors#

JET-EFDA, Culham Science Centre, OX14 3DB, Abingdon, UK
1) Istituto di Fisica del Plasma 'P.Caldirola', Associazione Euratom-ENEA-CNR, Milano, Italy
2) Max-Planck-Institut für Plasmaphysik, EURATOM Association, Garching, Germany
3) Università degli Studi di Milano, Dept. of Physics, Milano, Italy
4) Euratom/CCFE Association, Culham Science Centre, Abingdon, OX14 3DB, UK
5) FOM Institute Rijnhuizen, Association EURATOM-FOM, Nieuwegein, the Netherlands
6) Assoc. Euratom-IST, Instituto de Plasmas e Fusão Nuclear, Inst. Superior Técnico, Lisboa, Portugal
7) Association EURATOM - VR, Fusion Plasma Physics, EES, KTH, Stockholm, Sweden
8) CEA, IRFM, F-13108 Saint Paul Lez Durance, France
9) EFDA-CSU, Culham Science Centre, Abingdon, OX14 3DB, UK
10) LPP-ERM/KMS, Association Euratom-Belgian State, TEC, B-1000 Brussels, Belgium
11) Centre for Fusion Space and Astrophysics, University of Warwick, Coventry 7AL, UK
12) Association EURATOM-Tekes, Helsinki Univ. of Technology, FIN-02150 TKK, Finland
13) Association EURATOM-Hellenic Republic, Athens, Greece
14) Association EURATOM-Tekes, VTT, P.O. Box 1000, FIN-02044 VTT, Finland
15) Chalmers University of Technology and Euratom-VR Association, Göteborg Sweden
16) Consorzio RFX, ENEA-Euratom Association, Padua, Italy
17) Associazione EURATOM-ENEA sulla Fusione, C.R. Frascati, Frascati , Italy
18) Association Euratom-Risø DTU, DK-4000 Roskilde, Denmark
19) General Atomics, P.O. Box 85608, San Diego, California 92186-5608, USA
See Appendix of F.Romanelli et al., Overview of JET results, OV/1-3, this conference

E-mail contact of main author: mantica@ifp.cnr.it

Abstract. New experimental evidence indicates that ion stiffness mitigation in the core of rotating plasmas, observed previously in JET, results from the combined effect of high rotational shear and low magnetic shear. Ion stiffness in the outer plasma region is found to remain very high irrespective of rotation. Dedicated experiments in plasmas with different q profiles and rotation levels point to a larger effect of rotation in reducing stiffness when the core q profile is made flatter. The results have implications for the understanding of improved ion core confinement in hybrid plasmas or Internal Transport Barriers, both characterized by high rotation and low magnetic shear. Experimental evidence in these scenarios is discussed. Simulations indicate that the physics behind these results may lie in the ITG/TEM turbulence behavior at the transition between fully developed turbulence and zonal flows quenching. These findings point to the need for future devices of achieving sufficient rotational shear and capability of q profile manipulation to reach improved ion core confinement, which is an essential feature of Advanced Tokamak operation.

1.Introduction

Theoretical models of Ion Temperature Gradients (ITG) modes [1-4] indicate that ITGs feature a threshold in the inverse ion temperature gradient length ($R/L_{Ti}= R|\nabla T_i|/T_i$, with R the tokamak major radius) above which the ion heat flux (q_i) increases strongly with R/L_{Ti}. This property leads to a level of stiffness of T_i profiles, characterizing how strongly they are tied to the threshold. The role of plasma rotation on threshold and stiffness is of high relevance for predicting the performance of future devices, because the core T_i and fusion power achievable for a given T_i pedestal depend on threshold and stiffness [5] and future devices are expected to exhibit lower rotation than present devices from which scaling laws are derived.
The role of ExB flow shear stabilization [6] has been investigated in non-linear gyro-kinetic and fluid simulations with background flow [7-10] and comes out essentially as a threshold up-shift. From these studies the well-known quenching rule has been derived: $\gamma_{ExB}=\gamma_{noExB}-\alpha_E \omega_{ExB}$ where γ is the instability growth rate, ω_{ExB} is the flow shearing rate and $\alpha_E \sim 1$ (see [9] for a recent revision). Experimentally, the only study of the impact of rotation on ion threshold and stiffness was performed on JET (R=2.96m, a=1m)[11]. The unexpected result was

that in the core (ρ_{tor}=0.33) the main effect of rotation is to lower the ion stiffness, leading to high R/L_{Ti}, above the levels expected by the threshold up-shift given by the quenching rule. This paper presents new JET data on the combined role of rotation and magnetic shear. The new empirical hypothesis is proposed that the concomitant presence of high rotational shear and low magnetic shear is the condition for achieving ion stiffness mitigation in tokamaks. Dedicated experiments with q and rotation scans supporting such hypothesis are presented in Sect.2. The relevance of the observations with regard to improved ion core confinement as observed in JET Hybrid regimes [12] or ion Internal Transport Barriers (ITBs) [13] is examined in Sect.3 and 4. Initial attempts are then presented in Sect.5 to compare to experiment the predictions of state-of-art theory, discussing quasi-linear fluid and gyro-fluid and non-linear gyro-kinetic simulations.

2. Experimental investigation of ion heat transport

With reference to the main experiment discussed in [11] of q_i scan at ρ_{tor}=0.33 by varying the localization of ion ICH power in (^{3}He)-D minority, reported for sake of comparison in Fig.1a, the analysis of the data at ρ_{tor}=0.64 leads to Fig.1b, indicating that at outer radii the stiffness reduction due to rotation (observed at inner positions) is not present. The gyro-Bohm normalization is given by $q_i^{GB}= q_i\ [MW/m^2]/[(\rho_i/R)^2\ v_{ith}\ n_i\ T_i]$ with $v_{ith}=(T_i/m_i)^{1/2}$ and $\rho_i=(T_i/m_i)^{1/2}/eB$. That stiffness is always very high in the outer region is evident both from the q_i scan data and from T_i modulation data, which yield the slope of the curve as indicated by the two segments.

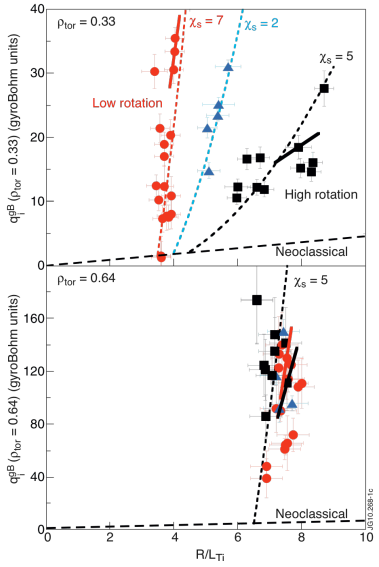

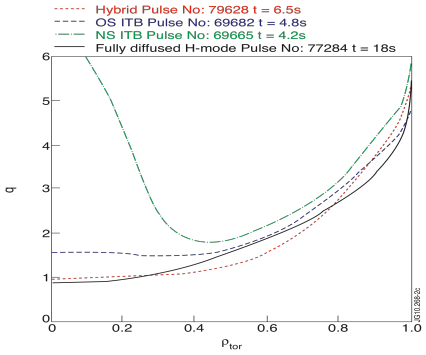

FIG.2: q profile reconstructed using EFIT constrained by MSE for typical JET discharges in different regimes: standard H-mode with fully diffused current profile, Hybrid, Optimized Shear ITB, Negative Shear ITB.

FIG.1: Gyro-Bohm normalized q_i vs R/L_{Ti} at (a) ρ_{tor}=0.33, (b) ρ_{tor}=0.64 for similar plasmas with different rotation levels. ●:1<ω_{t0}<2 10^4rad/s, ▲: 3<ω_{t0}<4 10^4rad/s, ■: 5<ω_{t0}<6 10^4 rad/s. The dashed black line is indicative of neoclassical transport. The 2 segments indicate the local slope deduced from modulation. The dotted lines represent the CGM curves with different values of χ_s.

Besides the higher values of normalized q_i in the outer region, a major difference in plasma parameters is the magnetic shear s=ρ/q dq/dρ. The rotational shear does not show a definite trend with radius. Fig.2 shows q profiles in 4 plasma regimes in JET, standard H-mode with fully diffused current profile (holding also for L-mode), hybrid, Optimized Shear (OS) ITBs and Negative Shear (NS) ITBs. The discharges contained in Fig.1 belong to the category of L-/H-modes (although mostly with early heating and non fully diffused q profile). Although the determination of s using magnetic and MSE or polarimeter data is affected by large uncertainties, we can say that in general s>1 at ρ_{tor}=0.64s whilst 0<s<0.5 at ρ_{tor}=0.33 for all types of discharges but the NS ITBs, where the low s is limited to a narrow layer around mid-radius. On the basis of Fig.1 we formulate a novel empirical hypothesis, that the stiffness reduction due to rotation as observed in [11] is only made possible by the concomitant presence of sufficiently low magnetic shear. Such hypothesis may have profound implications in the interpretation of the physics of improved ion core confinement as observed in Hybrid plasmas or ion ITBs, proposing an alternative paradigm to the usual interpretation in terms of ExB flow shear and threshold up-shift. In fact both regimes are observed to take place in

conditions of strong rotation and to be lost in absence of rotation [14,15]. An important role of q profile manipulation has been recognized in scenario development, with peculiar current waveforms inducing broad central regions of very low magnetic shear used to access hybrid regimes [16,17]; different ITB characteristics are observed in OS and NS ITBs, the first being broad regions whilst the second being narrow layers, in good match with the extension of the small s region [18,19,20] (although a role in many cases is also played by the higher neoclassical transport in the central region of NS plasmas); finally, in general it was found difficult to create ITBs in the external high magnetic shear region. These observations, although not directly proofing the stiffness reduction hypothesis, are nevertheless consistent with it, making mandatory a thorough experimental and theoretical investigation, in view of the implications for ITER Steady-State scenarios, which rely on improved ion core confinement.

A dedicated experiment aiming at studying the influence of s or s/q on ion threshold and stiffness in low and high rotation discharges has been performed. Ion threshold and stiffness have been measured as in [11] by scanning q_i with 3 MW on- and off-axis ICRH in (^{3}He)-D minority at concentrations n_{3He}/n_e~6-8% and measuring R/L_{Ti} with active Charge Exchange Spectroscopy. T_i modulation was performed on top. The low rotation discharges were identical to the ones shown with red circles in Fig.1, i.e L-mode, B_T =3.36 T, I_p=1.8 MA, n_{e0}=3–4 10^{19} m^{-3}. To induce rotation, up to 11 MW of co-injected NBI power was applied, and discharges were similar to those indicated as black squares in Fig.1. During the discharge time evolution, a scan of q profile was induced either by ramping I_p up and down between 1.8 and 3 MA within 3.5 s, or by adding Lower Hybrid power during the early pre-heat phase, or by applying the I_p overshoot recipe commonly used in hybrid regimes [17]. Current relaxation during and after these events provided a good range of q profiles, with s ranging between 0.05 and 0.8 (0.02<s/q<0.5) at ρ_{tor}=0.33 and between 0.75 and 1.45 (0.25<s/q<0.7) at ρ_{tor}=0.64. Fig.3a shows as an example the time evolution of the q profile in a low rotation shot with I_p ramp-up and off-axis ICRH. The time evolution of s and s/q at ρ_{tor}=0.33 and 0.64 are shown in Fig.3b. I_p ramp-up shots at high rotation show a similar q profile evolution, on a slightly slower time-scale due to higher temperatures. In low rotation discharges, positioning ICRH off-axis implies that the actual R/L_{Ti} at ρ_{tor}=0.33 is a measure of threshold, since q_i is close to zero. Therefore at low rotation the time evolution of R/L_{Ti} directly yields the dependence of threshold on s/q, which is expected from linear theory to play a stabilizing effect [21]. Fig.4 shows R/L_{Ti} vs time at ρ_{tor}=0.33 both for the low (77455) and high rotation (77477) I_p ramp-up shots, and also the prediction for the linear ITG threshold of 77477 using an analytical formula proposed in [21] in the flat density limit

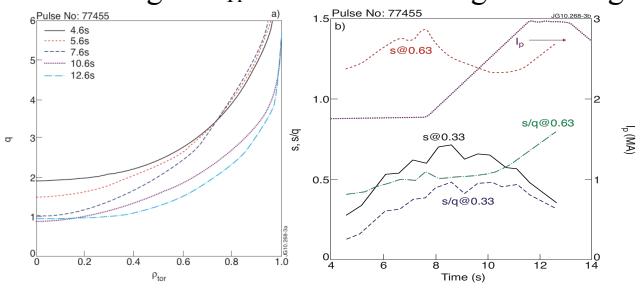

FIG.3: (a) time evolution of MSE q profile for a low rotation discharge with I_p ram-up; (b) I_p, s, s/q vs time at two radial positions.

$$R/L_{Ti}^{ITG} = \frac{4}{3}\left(1+\frac{T_i}{T_e}\right)\cdot\left(1+2\frac{s}{q}\right) \qquad \text{for} \qquad \frac{R}{L_n} < 2\left(1+\frac{T_i}{T_e}\right) \qquad (1).$$

The increase in measured threshold with time following the increase of s/q confirms the expected dependence of threshold on s/q and is in good match with Eq.(1) (low and high rotation shots do not differ substantially in linear threshold). In spite of such increase in threshold, however, it is remarkable that the time behaviour of R/L_{Ti} in the high rotation shot is opposite, with R/L_{Ti} lying 3 times above threshold in the early phase and drop ping to a factor 1.3 of threshold at late times. The value of s~0.7 measured at t~12 s, when the two shots become close, can be regarded as an estimate of the s value above which rotation no longer mitigates the ion stiffness. This seems confirmed by a preliminary analysis of the database of hybrid and H-mode plasmas presented in [33]. At low rotation also the on-axis ICRH case

(not shown, but virtually identical to the off-axis case) due to high stiffness keeps close to threshold with R/L_{Ti} increasing with time as expected. These observations constitute a beautiful confirmation of the fact that at high rotation the T_i dynamics is dominated by stiffness, and the stiffness reduction is more pronounced when the q profile is flatter (i.e. at early times). At outer radii, i.e. the high stiffness region, R/L_{Ti} both at low and high rotation keeps close to 7.5. Similar observations are made using the other schemes for q profile variation. These transport changes are accompanied by changes in turbulence as measured by correlation reflectometry. Two probing microwave beams are launched and the radial dial separation of their cutoff positions is scanned to obtain the reflectometer correlation length L [22]. Variations of L can result from changes in both the amplitude and the correlation length of the turbulence [23]. Fig. 5 shows at a given time lower L values for the high rotation pulse, for which larger flow shear decreases the turbulence correlation length, and consequently L. In time, a decrease of L is observed in the core for the high rotation pulse, but not at the outer plasma where L remains approximately constant. Since flow shear is stationary, this variation of L can be attributed to rising core turbulence [23], associated with increased transport. The observations are consistent with the changes observed in rotation and R/L_{Ti}.

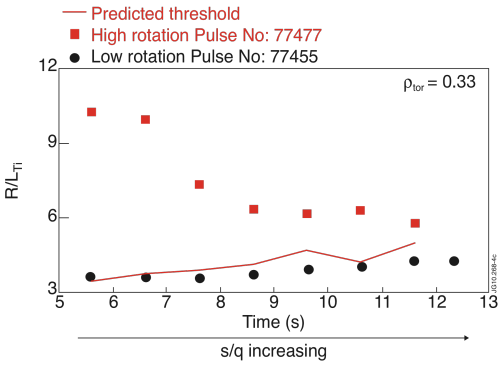

FIG.4: Experimental R/L_{Ti} at ρ_{tor}=0.33 vs time at low (black circles) and high (red squares) rotation for the I_p ramp-up case, and ITG threshold after Eq.(1) in the high rotation shot.

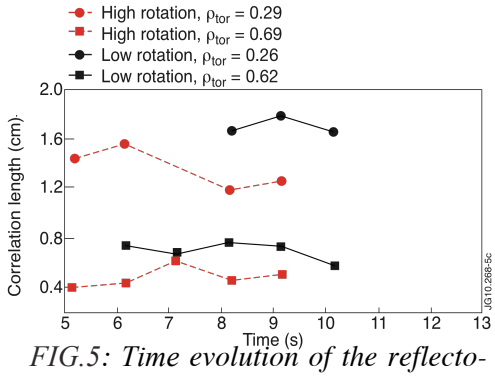

FIG.5: Time evolution of the reflectometer radial correlation length at two locations for the same shots of Fig.4.

One intriguing observation which is particularly clear in the example chosen is that the drop of R/L_{Ti} in time following the q profile relaxation between 5 and 9 s is not a continuous phenomenon, but takes place abruptly in time, around t=7 s, as can be seen from the T_i time traces in Fig.6a. A similar event takes place also at t=5.9 s but involving a smaller central region, therefore not affecting the R/L_{Ti} at ρ_{tor}=0.33 in Fig.4. T_i profiles before and after t=7s are compared in Fig.6b, showing that the decrease of stiffness at ρ_{tor}=0.33 is to be interpreted as a shrinking in space of the core low stiffness region. The increase of stiffness in the core is evidenced by the remarkable change in slope of the modulation phase profiles, shown in Fig.7 for a similar discharge. It has been verified that no MHD mode sets in at t=7s, which could produce the abrupt local flattening of T_i. On the contrary, a m=2, n=1 is clearly present between t=6.2 s and t=7 s in the region ρ_{tor} =0.3-0.4. Such mode is not big enough to affect the T_i profile, and stops completely at t=7 s. Therefore the T_i modification at t=7 s is not to be linked to MHD

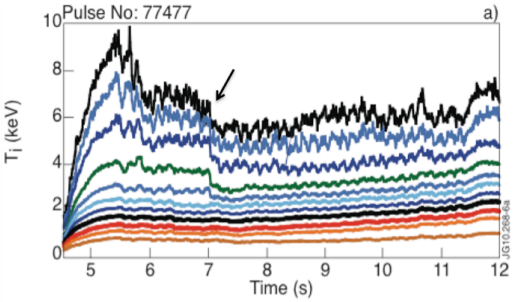

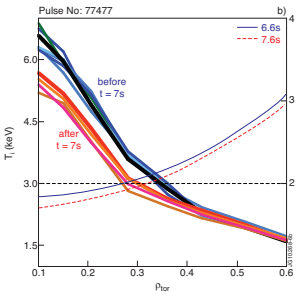

FIG.6: Experimental T_i at different radii vs time(a) and vs ρ_{tor} (b)together with q for the high rotation discharge 77477.

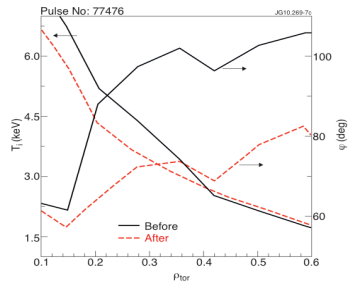

FIG.7: Profiles of T_i and T_i modulation phase before and after the shrinking event for the high rotation discharge 77476.

phenomenology. It is possible however that it has to do with the movement of the q=2 surface from low to higher shear region, which stabilizes the MHD mode but turns out to deteriorate transport, determining the erosion of the low stiffness region. This is actually in line with various experimental observations of the beneficial role of low order rationals near s=0 on turbulent transport [24-27], for which a theoretical basis was proposed in [28].

3. The physics of Hybrid and ITB plasmas

An effort has been made to investigate if stiffness mitigation is at work also in high performance hybrid and ITB plasmas, and to what extent it contributes to global confinement. When examining their position in the q_i^{GB} vs R/L_{Ti} plot (Fig.8, including for comparison the data of Fig.1a through its CGM fits), one realizes that high values of R/L_{Ti} are achieved in presence of low q_i^{GB}. It has been verified using GS2 [29] that the linear threshold lies between 3.5 and 5, i.e. not significantly increased with respect to the value found for the discharges of Fig.1a.

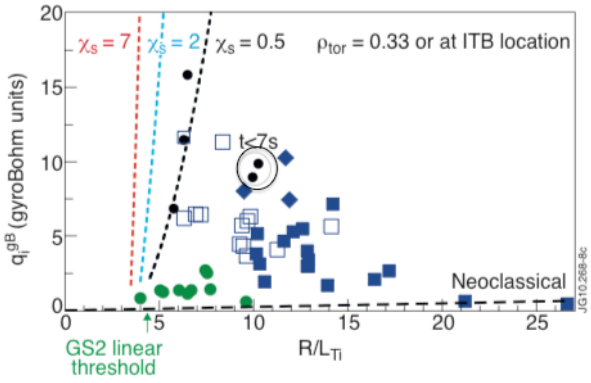

FIG.8: q_i^{GB} vs R/L_{Ti} at ρ_{tor}=0.33 for a set of Hybrid plasmas (green circles), ion ITBs at trigger time (blue open squares) and fully developed (blue full squares, diamonds with large ICRH fraction and reduced rotation). The location of the data of Fig.1a is shiwn by their CGM fits. Neoclassical level and GS2 linear threshold for a representative hybrid case are indicated.

In hybrids, the rotation has high values but still smooth profiles, the flow shearing rate is in the order of 3-4 10^4 s^{-1}, not enough to produce large threshold up-shifts. So the profiles lie well above threshold even if q_i^{GB} is small, indicating low stiffness. This is actually consistent with measurements of the level of stiffness made using NBI T_i modulation (^{3}He ICRH heating is not available due to low B_T) and changes in q_i^{GB} by degrading the pedestal T_i with enhanced B_T ripple [30]. In both cases (although for lack of space we cannot show here the details) the plasma behavior was found consistent with low ion stiffness level in a core region that could expand up to ρ_{tor}=0.6. In the outer region the stiffness level is as usual very high, with R/L_{Ti} values similar to those in Fig.1b. A clear effect of rotation on R/L_{Ti} has also been recognized when comparing low and high triangularity hybrid plasmas, the latter having in general lower rotation due to higher density, as discussed in [31]. For ITBs, the discussion on the role of ExB shearing requires a distinction between the profiles at trigger time and during the phase of fully developed ITBs, both shown in Fig.8. In the first case, ω_{ExB} is still in the range of 1-2 10^4 s^{-1}, not producing a significant threshold up-shift, and the data lie in a stiffness region intermediate between the rotating shots of Fig.1a and the neoclassical level. In the fully developed ITB however, particularly in the NS case, the ITB itself generates a large and localized rotation gradient at ITB location, which implies values of ω_{ExB} up to 7-8 10^4 s^{-1}, inducing through the Waltz rule significant threshold upshifts. In such situation it is difficult to separate the role of threshold and stiffness. Therefore, T_i modulation has been performed using ^{3}He ICRH modulation, as shown in Fig.9, which compares the amplitude profiles with and without well developed ITB, respectively for a case of narrow ITB with RF deposition at ITB location, and for a case of broad ITB with RF deposition on-axis. It is visible that the ITB acts as a layer of very low incremental diffusivity, producing a sharp variation of amplitudes with respect to a similar plasma with identical RF deposition but no ITB. This implies a very low slope of the q_i vs R/L_{Ti} plot. Analogous observations were reported for electrons in [32]. This is not consistent with being tight to a high threshold by high stiffness. It would be consistent both with a picture of transport above critical but with very low stiffness, or of a subcritical transport, i.e. plasma getting below threshold due to a very large threshold up-shift. However the second situation must be discarded because as

seen in Fig.8 in most cases both ITBs and hybrids are found significantly above the neoclassical level. Given the continuous pattern of decreasing stiffness in Fig.1a and 8, it is natural to argue that also in fully developed ion ITBs the mechanism of stiffness mitigation plays a major role, with the threshold up-shift intervening in a non-linear feedback whilst the ITB develops. Therefore the picture for ions would be rather different from that for electrons proposed in [32], with electron ITBs as sub-critical regions in presence of stiff electron transport. A confirmation of such difference comes from the different behavior of electron and ion cold pulses when they meet the ITB propagating from edge (Fig.10). In the electron case, the cold pulse grows significantly inside the ITB layer [32], which was interpreted and modeled [33] in terms of a re-destabilization of turbulent transport due to the increased R/L_{Te} carried by the cold pulse, with leads above threshold and in presence of stiff electron transport causes a significant increase in electron diffusivity. For ions, whose stiffness is low in the ITB region, such cold pulse growth should not be possible, which is confirmed experimentally in Fig.10. One can see that the ion cold pulse is strongly damped in the ITB region, without experiencing the large growth seen in the electron cold pulse. We notice that the smaller growth outside the ITB both of ion and electron cold pulse is a different phenomenon associated to a convective-like effect in the presence of stiff transport as discussed in [33].

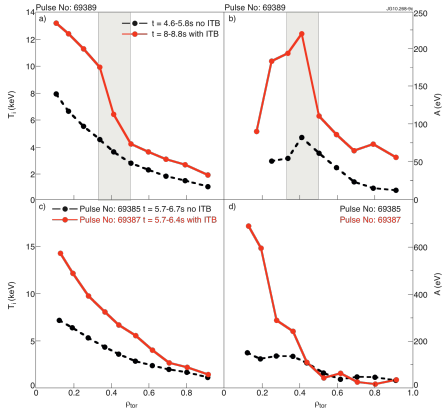

FIG.9: T_i (left) and amplitude (right) profiles for an ITB discharge before ITB triggering (black dashed line) and at full development (red full line), for a narrow ITB with RF at ITB location (top) and a broad ITB with on-axis RF (bottom).

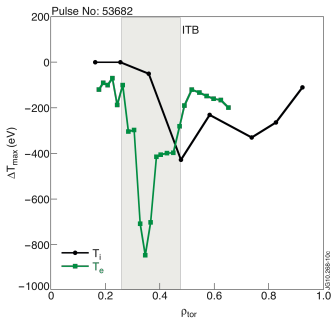

FIG.10: Cold pulse maximum amplitude for ions and electrons. The ITB region is marked.

4. Impact of ion stiffness mitigation on scenario performance

While it is clear that in ITB plasmas the enhancement in H factor up to ~1.5 is completely due to the onset of large core gradients, without any significant change of the edge, in the case of hybrid plasmas there are other mechanisms that contribute to increase the H factor to ~1.3-1.5, namely the enhanced pedestal and the stabilization of the NTMs which are often acting in standard H-modes. The pedestal enhancement has a larger impact on global confinement than the core enhancement, due to volume effects, although fusion power, being dependent on core T_i, benefits in larger measure than confinement from a core improvement. It has been shown statistically over a large database [34] that the contribution of pedestal energy to total energy is 20-40% both in H-modes and in hybrids and that the improvement of H factor up to 1.5 in hybrids is due in equal parts to core and pedestal improvement and is mainly located in the ion channel. This equal repartition is consistent with the situation in which R/L_{Ti} is preserved in presence of an increased pedestal. On the other hand, there are also cases as seen in Fig.8 in which R/L_{Ti} increases, with a higher gain in the core part. We estimate that an improvement in R/L_{Ti} from 6 to 10 in a region up to ρ_{tor} =0.6 at fixed pedestal leads to an enhancement of H factor by ~0.2. Therefore the stiffness

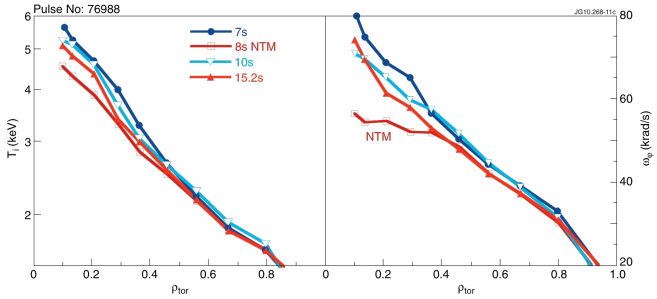

FIG.11: (a) T_i and (b) angular frequency profiles for a long hybrid like pulse. A strong NTM is developed around 8 s but fades out at later times.

variations described in this paper can play a role also on global performance if the region of flat q can be extended to large radii. With regard to NTMs, the experiments show [35] that NTM onset leads to an abrupt drop of the H factor. Part of this drop can be attributed to a change in R/L_{Ti}, which is mainly caused by the braking of plasma rotation, as can be seen in Fig.11. It is important to notice, also in Fig.11, that once the NTM has weakened and rotation and T_i profile have recovered, the same core T_i dynamics described previously, showing a shrinking of the high R/L_{Ti} (low stiffness) region in time, can also be observed in hybrids.

5. The impact of rotation in theory

Finally, we address the issue of theory predictions of the effect of rotation on ion transport. This is discussed on the basis of Figs.12 a-b, which show q_i^{GB} vs R/L_{Ti} at different values of rotation ($\gamma_E=\omega_{ExB}/(c_s/a)$, with $c_s=\sqrt{(T_e/m_i)}$) for scans in R/L_{Ti} performed a) without collisions and keeping R/L_{Te} fixed; b) with electron collisions and varying R/L_{Te} in a prescribed ratio with R/L_{Ti}. The latter case is nearest to experimental conditions. Widely used quasi-linear transport models, such as Weiland [36] or GLF23 [37], have been found not able to reproduce the results shown in Fig.1, since rotation implies only a (small) threshold up-shift and not a change in slope. This is possibly due to application of the Waltz rule to a reduced selection of wavelengths in the turbulence spectrum. The results from the Weiland model are shown in Fig.12b for different rotation levels up to the experimental level of the high rotation cases of Fig.1 (γ_E=~0.1). A set of non-linear gyro-kinetic simulations with the set of assumptions (a) using GKW [38], which includes background rotation, have been performed starting from the parameters of one high rotation discharge and are shown in Fig.12a. These seem to indicate again also only a threshold up-shift, even extending to large values γ_E~0.2. A set of simulations using the gyro-fluid TGLF model [39] under the same assumptions (a) is also shown in Fig.12a. Here we started from the parameters of one low rotation discharge in order to verify that the small changes of other parameters between low and high rotation shots were not the cause of the different stiffness, which is the major effect that we ascribe to rotation. In fact the two curves at γ_E=0 agree pretty well between the two models, implying that the slightly different set of parameters plays a minor role with respect to the effect we are studying. The TGLF simulations in Fig.12a show that, whilst at large flux values the stiffness level is not changed significantly by rotation, in the region of the knee, where the transition between fully developed turbulence and zonal flows quenching takes place, the slope of the curves is significantly affected by rotation. This effect is possibly due to differential suppression of turbulence at various wavelengths in the spectrum, with more suppression of the low stiffer wavelengths. Such bending of the curve may missed in the GKW result due to the coarse grain in R/L_{Ti}, associated with the higher demand of computing time.

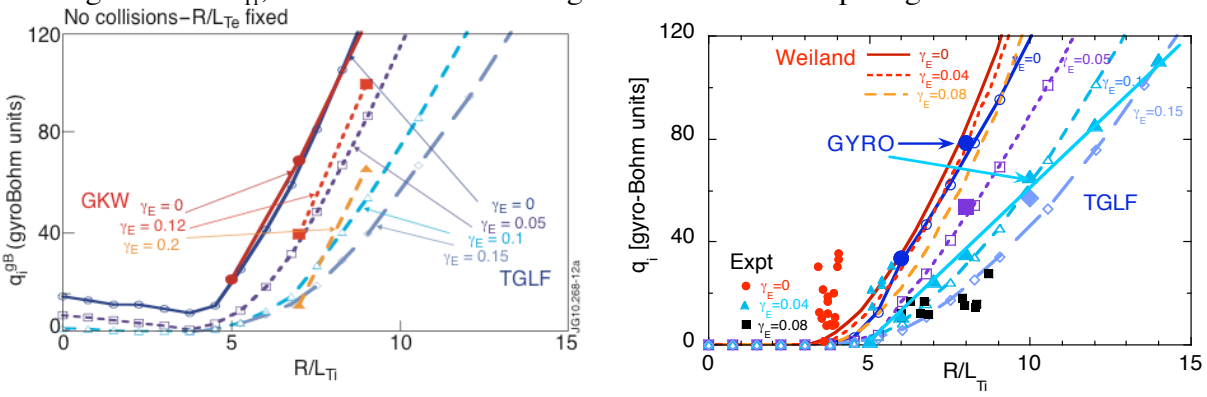

FIG.12: q_i^{GB} vs R/L_{Ti} at ρ_{tor}=0.33 using the parameters of one shot from Fig.1 and different rotation levels a) from a set of collisionless GKW (non-linear) and TGLF simulations, keeping R/L_{Te} fixed; b) from Weiland model, TGLF and GYRO (non-linear) simulations including electron collisions and varying R/L_{Te} in a fixed ratio with R/L_{Ti}. In b) also the experimental data of FIG.1a are shown.

A set of TGLF simulations under the assumptions (b), closer to experiment, is shown in Fig. 12b. The effect of rotation on the slope of the TGLF curves is even stronger, especially in the knee region, and resembles also quantitatively what is observed in experiment. A set of non-linear GYRO [40] runs in Fig.12b also shows the effect of rotation on slope, although without much evidence of a knee region. We conclude that the experimental evidence on the effect of rotation on ITG/TEM modes in the region close to threshold, where future machine will operate, is in fair agreement with theory predictions provided that the full turbulence spectrum is taken into account. This topic will deserve more detailed studies, possibly also including the role of rational surfaces and extending to global, non-linear, fixed flux ITG turbulence codes.

It is worth noting that non-linear fluid simulations of resistive ballooning modes (RBM), which have essential features common with ITGs, indicated [41] an effect of rotational shear also on stiffness. This has however not been confirmed by recent RBM simulations in [42].

6. Conclusions

In summary, we have presented experimental evidence that ion stiffness is reduced by the combined effect of low magnetic shear and high rotational shear, which bears the indication that AT scenarios in ITER should seek for maximum rotational shear compatible with the available heating systems and minimum magnetic shear in the broadest region to enhance the rotational shear effect. Some initial theory investigations point to an effect of rotation on stiffness at low normalized heat flux, in the transition region between fully developed turbulence and zonal flows quenching, which is the domain of operation of fusion relevant devices. This calls for further theory work, in particular on the interplay of rotation with magnetic shear and rational surfaces.

This work, supported by the European Communities under the contract of Association EURATOM/ ENEA-CNR, was carried out within the framework of EFDA. The views and opinions expressed herein do not necessarily reflect those of the European Commission.

References

[1] MATTOR, N., et al., Phys. Fluids **31** (1988) 1180
[2] ROMANELLI,F., et al.,Phys.Fluids B **1**(1989)1018
[3] CONNOR, J.W. and WILSON, H.R., Plasma Phys. Controlled Fusion **36** (1994) 719
[4] KOTSCHENREUTHER, M., et al., Phys. Plasmas **2** (1995) 2381
[5] BAIOCCHI, B., et al., in preparation
[6] BIGLARI, H., et al., Phys. Fluids B **2** (1990) 2
[7] KINSEY,J.E.,et al.,Phys.Plasmas **12** (2005) 062302
[8] WALTZ, R.E., et al., Phys. Plasmas **1** (1994) 2229
[9] KINSEY,J.E.,et al.,Phys.Plasmas **14** (2007) 102306
[10] GARBET, X., et al., Phys. Plasmas **9** (2002) 3893
[11] MANTICA, P.et al., Phys. Rev. Lett. **102** (2009) 175002
[12] IMBEAUX, F., et al., Plasma Phys. Control. Fusion **47** (2005) B179
[13] WOLF, R.C., Plasma Phys. Control. Fusion **45** (2003) R1
[14]DE VRIES,P.C.,et al,Nucl.Fusion **49**(2009)075007
[15]POLITZER,P.A.et al,Nucl.Fusion**48** (2008)075001
[16] WADE, M.R., et al., Nucl. Fusion **45** (2005) 407
[17] HOBIRK,J.,et al., in press
[18] LITAUDON,X.,et al., EXC/P4-12, this conference
[19] SAKAMOTO,Y., et al., Nucl. Fusion **49** (2009) 095017
[20] SUZUKI,T., et al.,Nucl. Fusion **49** (2009) 085003
[21] GUO, S.C., et al., Phys. Fluids B **5** (1993) 520
[22] FIGUEIREDO, A.C.A., et al., Rev. Sci. Instrum. **79**, (2008) 10F107
[23] FIGUEIREDO, A.C.A., et al., 36th EPS Conf. on Plasma Phys., Sofia, 2009 ECA Vol.33E, P-2.167 (2009)
[24] LOPES CARDOZO, N.J., et al., Plasma Phys. Control. Fusion **39** (1997) B303
[25] AUSTIN, M.E., et al., Phys. Plasmas **13** (2006) 082502
[26] JOFFRIN,E., et al., Nucl. Fusion **43** (2003) 1167
[27] JOFFRIN,E., et al., Nucl. Fusion **42** (2002) 235
[28] WALTZ,R.E.,et al.,Phys.Plasmas **13**(2006)052301
[29]KOTSCHENREUTHER, M., et al., Comput. Phys. Commun. **88** (1995) 128
[30]SAIBENE,G.,et al.,Proc. 22nd IAEA Fusion Energy Conference,Geneva,2008 (IAEA,Vienna, 2008) EX/2-1
[31] JOFFRIN, E., et al., EX/1-1, this conference
[32] MANTICA, P., et al., Phys. Rev. Lett. **96** (2006) 095002
[33] CASATI,A., et al., Phys.Plasmas **14**(2007)092303
[34]FRASSINETTI, L., et al., 37th EPS Conference on Plasma Phys. Dublin, 2010, P-1.1031
[35] CHALLIS,C.D. et al.,36th EPS Conference on Plasma Phys.Sofia,2009, ECA Vol.**33E**,P-5.172 (2009)
[36] WEILAND,J., *Collective Modes in Inhomogeneous Plasmas* (IOP, Bristol, 2000)
[37] WALTZ,R.E.,et al., Phys. Plasmas, **4** (1997) 2482
[38] PEETERS, A.G., et al., Comput. Phys. Commun. **180** (2009) 2650
[39] STAEBLER, G.M., et al., Phys. Plasmas **14** (2007) 055909
[40] CANDY,J. and WALTZ, R.E., J. Comput. Phys. **186** (2003) 545
[41] FIGARELLA, C.F., et al., Phys. Rev. Lett. **90** (2003) 015002
[42] SUGITA, S., et al., 37th EPS Conference on Plasma Phys. Dublin, 2010, P1.1095 (2010)